

# Physical Origin of the Opsin Shift of Bacteriorhodopsin. Comprehensive Analysis Based on Medium Effect Theory of Absorption Spectra

Hirohiko Houjou, Yoshio Inoue, and Minoru Sakurai\*

Contribution from the Department of Biomolecular Engineering, Tokyo Institute of Technology,  
4259 Nagatsuta-cho, Midori-ku, Yokohama 2268501, Japan

Received November 17, 1997. Revised Manuscript Received March 9, 1998

**Abstract:** To elucidate the origin of the opsin shift of bacteriorhodopsin (bR), a self-consistent reaction field method combined with configuration interaction calculation is employed. In addition, the absorption maxima of *all-trans*-retinal and its Schiff bases are measured in a variety of aprotic solvents. It is shown that the calculation reproduces well the observed solvatochromic shifts. From regression analysis, we obtain an empirical relationship between the absorption maximum of protonated retinal Schiff base and physical parameters of solvent, including dielectric constant and refractive index. On the other hand, based on the crystal structure of bR, we estimate the effective values of such parameters for the retinal-binding pocket. Combining these results, it is shown that the opsin shifts of bR<sub>568</sub> and M<sub>412</sub> can be quantitatively reproduced if the protein matrix acts as a polarizable medium with a high refractive index. From decomposition analysis of the calculated opsin shift, the contributions of (i) ring/chain coplanarization, (ii) separation of a counterion, and (iii) medium effects of the protein are shown to be 2500, 1200, and 1000 cm<sup>-1</sup>, respectively. It is revealed that the effects (i) and (ii) are independent of each other, but the effects (ii) and (iii) are significantly correlated. In a polarizable medium, a shift induced by a counterion is almost canceled out by an opposite shift induced by medium effects. In conclusion, the polarizable medium effects play a decisive role in the wavelength regulation of bR.

## Introduction

Bacteriorhodopsin (bR) is a retinal-bound protein and functions as a light-driven proton pump in the purple membrane of *Halobacterium salinarium*.<sup>1</sup> Illumination of the light-adapted state bR<sub>568</sub> initiates a sequential photoreaction cycle consisting of the spectroscopically distinct intermediates K<sub>610</sub>, L<sub>550</sub>, M<sub>412</sub>, N<sub>520</sub>, and O<sub>640</sub>.<sup>2</sup> In the initial state bR<sub>568</sub>, the chromophore retinal takes *all-trans* form and is bound to Lys216 residue via protonated Schiff base linkage. The absorption maximum of bR<sub>568</sub> is 568 nm, which is significantly red shifted in comparison with that of protonated retinylidene Schiff base (PRSB) measured in methanol solution (~440 nm). In the M<sub>412</sub> state, the chromophore undergoes *all-trans* → 13-*cis* isomerization, and loses its Schiff base proton. Being similar to bR<sub>568</sub>, the absorption maximum of M<sub>412</sub> is red shifted with respect to the corresponding solution data. Similar phenomena are also observed in visual pigments. Rhodopsin (Rh), the rod pigment of vertebrate, contains the chromophore 11-*cis*-retinal, which shows the absorption maximum at ~500 nm.<sup>1</sup> Such protein-induced bathochromic shifts are known as opsin shift.<sup>1</sup> The elucidation of its mechanism has been an interesting issue in photochemistry of retinal-bound proteins for these decades.

The opsin shift is considered to arise mainly from the following three factors: elongation of the  $\pi$ -conjugated system due to the ring/chain coplanarization, hereafter called mechanism (1);<sup>3–6</sup>  $\pi$ -electron delocalization due to weakening of the interaction between PRSB and its counterion (mechanism (2));<sup>7,8</sup> interaction of the chromophore with polar or polarizable residues in the protein. Among them, the molecular detail of the third factor remains unclear, although much effort has been made to identify the chromophore–protein interactions directly responsible for the opsin shift. There are two conceptual models for this factor. One is the so-called external point charge model (mechanism (3)) proposed by Nakanishi's group.<sup>9</sup> The other model emphasizes the electronic polarization effect of aromatic residues (mechanism (4)).<sup>10</sup>

(3) van der Steen, R.; Biesheuvel, P. L.; Mathies, M. A.; Lugtenburg, J. *J. Am. Chem. Soc.* **1986**, *108*, 6410.

(4) Harbison, G. S.; Smith, S. O.; Pardo, J. A.; Courtin, J. M. L.; Lugtenburg, J.; Herzfeld, J.; Mathies, R. A.; Griffin, R. G. *Biochemistry* **1985**, *24*, 6955.

(5) Harbison, G. S.; Mulder, P. P. J.; Pardo, H.; Lugtenburg, J.; Herzfeld, J.; Griffin, R. G. *J. Am. Chem. Soc.* **1985**, *107*, 4809.

(6) Wada, M.; Sakurai, M.; Inoue, Y.; Tamura, Y.; Watanabe, Y. *J. Am. Chem. Soc.* **1994**, *116*, 1537.

(7) Bassov, T.; Sheves, M. *J. Am. Chem. Soc.* **1985**, *107*, 7524.

(8) (a) Blatz, P. E.; Johnson, R. H.; Mohler, J. H.; Al-Dilaimi, S. K.; Dewhurst, S.; Erickson, J. O. *Photochem. Photobiol.* **1971**, *13*, 237. (b) Blatz, P. E.; Mohler, J. H.; Navanglu, H. V. *Biochemistry* **1972**, *11*, 848. (c) Blatz, P. E.; Mohler, J. H. *Biochemistry* **1972**, *11*, 3240. (d) Blatz, P. E.; Mohler, J. H. *Biochemistry* **1975**, *14*, 2340.

(9) (a) Arnaboldi, M.; Motto, M. G.; Tsujimoto, K.; Balogh-Nair, V.; Nakanishi, K. *J. Am. Chem. Soc.* **1979**, *101*, 7082. (b) Honig, B.; Dinur, U.; Nakanishi, K.; Balogh-Nair, V.; Gawinowics, M. A.; Arnaboldi, M.; Motto, M. G. *J. Am. Chem. Soc.* **1979**, *101*, 7084. (c) Sheves, M.; Nakanishi, K.; Honig, B. *J. Am. Chem. Soc.* **1979**, *101*, 7086.

\* To whom all correspondence should be addressed.

(1) See for reviews: (a) Birge, R. R. *Annu. Rev. Phys. Chem.* **1990**, *41*, 683. (b) Lanyi, J. K. *Biochim. Biophys. Acta* **1993**, *1183*, 241. (c) Nathans, J. *Biochemistry* **1992**, *31*, 4923. (d) Khorana, H. G. *Ann. N. Y. Acad. Sci.* **1986**, *471*, 272. (e) Mathies, R. A.; Lin, S. W.; Ames, J. B.; Pollard, W. T. *Annu. Rev. Biophys. Chem.* **1991**, *20*, 491. (f) Nakanishi, K. *Pure Appl. Chem.* **1991**, *63*, 161. (g) Ottolenghi, M.; Sheves, M. *J. Membr. Biol.* **1989**, *112*, 193.

(2) Lozier, R.; Bogomolni, R. A.; Stoekenius, W. *Biophys. J.* **1975**, *15*, 955.

The location of the external charge has been intensively explored by a series of experiments using artificial pigments reconstituted with dehydro- or dihydroretinals.<sup>9,11–15</sup> For bR, a negatively charged or polar residue has been proposed to be present near the  $\beta$ -ionone ring.<sup>12,16</sup> Such a residue would largely delocalize the  $\pi$ -electrons of the chromophore, resulting in a significant amount of red shift. This mechanism was partially supported by experiments using model compounds which possess charged groups covalently bound to retinal itself.<sup>7,17,18</sup> However, there is room for argument against mechanism (3). First, this cannot account for the spectral shift of  $M_{412}$ .<sup>19</sup> Second, from the crystal structure at 3.5 Å resolution,<sup>20</sup> such external charge(s) could not be identified. In addition, from a series of mutagenetic studies, it was shown that any ionizable residues do not contribute to the bathochromic shift observed in the wild-type bR.<sup>21</sup> As for Rh, it has been also proposed that a second (i.e., other than the counterion of PRSB) negative charge is present near C12 and C14 of the chromophore (For the numbering of carbon atoms, see Figure 1.)<sup>9</sup> Later, results from two-photon spectroscopy indicated that the chromophore-binding site is electrically neutral, suggesting the absence of the second negative charge.<sup>22</sup> Thus, the importance of mechanism (3) is currently open to question.

According to mechanism (4),<sup>10</sup> the occurrence of the bathochromic shift is explained as follows. The dipole moment of PRSB in the lowest  $\pi$ - $\pi^*$  excited state is larger than that in the ground state.<sup>23</sup> The surrounding solvent molecules could be electronically repolarized in response to the change in electronic distribution of the solute molecule. Such a solvent relaxation contributes to stabilizing the excited state, resulting in a red shift. In proteins, aromatic amino residues (phenylalanine, tyrosine and tryptophan) would play a role similar to polarizable solvents.<sup>22,24</sup> This mechanism is supported by the fact that the absorption maximum of PRSB in ethanol shifts to red-side by addition of phenol, indole, etc.<sup>25</sup>

In view of accumulated evidence, the whole opsin shift may not be reproduced only by the single action of any one of the

(10) (a) Irving, C. S.; Byers, G. W.; Leermakers, P. A. *J. Am. Chem. Soc.* **1969**, *91*, 2141. (b) Irving, C. S.; Byers, G. W.; Leermakers, P. A. *Biochemistry* **1970**, *9*, 858.

(11) Honig, B.; Greenberg, A. D.; Dinur, U.; Ebrey, T. G. *Biochemistry* **1976**, *15*, 4593.

(12) (a) Nakanishi, K.; Balogh-Nair, V.; Arnaboldi, M.; Tsujimoto, K.; Honig, B. *J. Am. Chem. Soc.* **1980**, *102*, 7945. (b) Motto, M. G.; Sheves, M.; Tsujimoto, K.; Balogh-Nair, V.; Nakanishi, K. *J. Am. Chem. Soc.* **1980**, *102*, 7947.

(13) Mao, B.; Govindjee, R.; Ebrey, T.; Arnaboldi, M.; Balogh-Nair, V.; Nakanishi, K. *Biochemistry* **1981**, *20*, 428.

(14) Spudich, J. L.; McCain, D. A.; Nakanishi, K.; Okabe, M.; Shimizu, N.; Rodman, H.; Honig, B.; Bogomolni, A. *Biophys. J.* **1986**, *49*, 479.

(15) Koutalos, Y.; Derguini, F.; Tsuda, M.; Odashima, K.; Lien, T.; Park, M. H.; Shimizu, N.; Derguini, F.; Nakanishi, K.; Gilson, H. R.; Honig, B. *Biochemistry* **1989**, *28*, 2732.

(16) Lugtenburg, J.; Muradin-Szweykowska, M.; Heeremans, C.; Pardo, J. A.; Griffin, R. G.; Smith, S. O.; Mathies, R. A. *J. Am. Chem. Soc.* **1986**, *108*, 3104.

(17) Sheves, M.; Nakanishi, K. *J. Am. Chem. Soc.* **1983**, *105*, 4033.

(18) Derguini, F.; Caldwell, C. G.; Motto, M. G.; Balogh-Nair, v.; Nakanishi, K. *J. Am. Chem. Soc.* **1983**, *105*, 646.

(19) Gat, Y.; Sheves, M. *Photochem. Photobiol.* **1994**, *59*, 371.

(20) Grigoroff, T.; Ceska, K.; Downing, K. H.; Baldwin, J. M.; Henderson, R. *J. Mol. Biol.* **1996**, *259*, 393.

(21) Mogi, T.; Stern, L. J.; Marti, T.; Chao, B. H.; Khorana, H. G. *Proc. Natl. Acad. Sci. U.S.A.* **1988**, *85*, 4148.

(22) Birge, R. R.; Murray, L. P.; Pierce, B. M.; Akita, H.; Balogh-Nair, V.; Findsen, L. A.; Nakanishi, K. *Proc. Natl. Acad. Sci. U.S.A.* **1985**, *82*, 4117.

(23) Mathies, R.; Stryer, L. *Proc. Natl. Acad. Sci. U.S.A.* **1976**, *73*, 2169.

(24) Suzuki, T.; Kito, Y. *Photochem. Photobiol.* **1972**, *15*, 275.

(25) (a) Kliger, D. S.; Milder, S. J.; Dratz, E. A. *Photochem. Photobiol.* **1977**, *25*, 277. (b) Milder, S. J.; Kliger, D. S. *Photochem. Photobiol.* **1977**, *25*, 287.

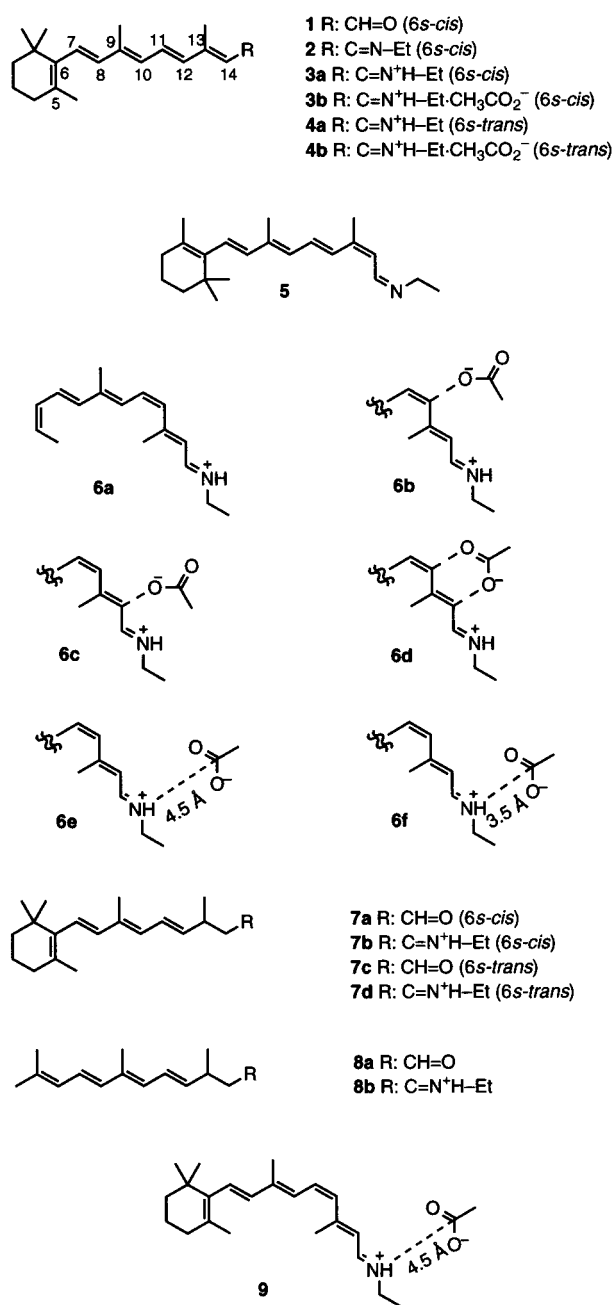


**Figure 1.** Molecular structures of *all-trans*-retinal and its related compounds.

four mechanisms. More current view of the spectral tuning mechanism stresses the necessity of concerted action of some of them. There were several attempts to decompose the opsin shift into a couple of contributions. Recently, Yan et al.<sup>26</sup> reported the results of experiments using 13,14-dihydro-analogues. The use of these analogues allows one to exclude the contribution of PRSB-counterion interaction (mechanism (2)) to the entire bathochromic shift. They concluded that mechanisms (3) and/or (4) actually work in bR, and their net contribution amounts to a red shift of 2030  $\text{cm}^{-1}$ . On the other hand, according to a report of Hu et al.,<sup>27</sup> each of the mechanisms (1) and (2) causes a red shift of about 2000  $\text{cm}^{-1}$ . They proposed that the cooperative action of the models (1)

(26) Yan, B.; Spudich, J. L.; Mazur, P.; Vunnam, S.; Dergini, F.; Nakanishi, K. *J. Biol. Chem.* **1995**, *270*, 29668.

(27) Hu, J.; Griffin, R. G.; Herzfeld, J. *Proc. Natl. Acad. Sci. U.S.A.* **1994**, *91*, 8880.

and (2) causes an additional red shift ( $\sim 1000 \text{ cm}^{-1}$ ), leading to full reproduction of the observed opsin shift without requiring mechanisms (3) and (4).

Therefore, the mechanism of the opsin shift is still controversial. For a comprehensive understanding of it, one must accurately evaluate the individual contributions of (1)–(4) and their cooperative action. Among them, (1)–(3) have been well investigated from both experimental and theoretical viewpoints.<sup>28–30</sup> However, the polarizable effect of the protein environment, i.e., the mechanism (4), has not been quantitatively studied so far.

Quantum chemical calculation is expected to provide a good insight into the above problem if a sophisticated solvent model is available. Self-consistent reaction field polarizable continuum model (SCRFP-PCM)<sup>31</sup> is a reliable approximation to implement dielectric solvent effects into molecular orbital calculation. Raudino et al.<sup>32</sup> applied a SCRFP-PCM to analysis of environmental effects on a PRSB-counterion system. However, due to methodological limitation in their SCRFP model, that report dealt with only two limiting cases: (i) dielectric constant equals the square of refractive index, and (ii) refractive index equals 1. The cases (i) and (ii) correspond to the conditions under which the relaxation of electronic polarization is infinitely fast and slow, respectively, while the actual situation lies between these two cases. In addition, they used a spherical cavity to accommodate the PRSB-counterion system. The use of a cavity which does not fit a molecular shape might lead an error in evaluating medium effects. Furthermore, the use of a cavity with a fixed shape and size could not allow one to correctly follow effects of structural changes of the solute, including changing location of the counterion.

The evaluation of solvatochromic shifts of molecules is a topical subject of theoretical chemistry.<sup>31</sup> Recently, we have developed a new SCRFP-PCM theory, capable of calculating medium effects with taking into account both orientational and electronic polarization effects of solvent.<sup>33</sup> Namely, excitation energy is given as a function of dielectric constant and refractive index. This method can handle an arbitrarily shaped cavity, because its formulation was based on the boundary element method.<sup>34</sup> Its application to a merocyanine dye molecule successfully reproduced the solvatochromic shift observed in a variety of solvents.<sup>33</sup> Therefore, our method has overcome the disadvantages of the previous solvent model and hence is promising for unraveling the mechanism of the opsin shift.

In this study, our SCRFP-CI method is applied to the problem of opsin shift. It is shown that the calculation excellently reproduces solvatochromic shifts observed for *all-trans*-retinal and its Schiff bases. By regression analysis, we obtain an empirical equation to predict solvatochromic shifts of PRSB for an arbitrary set of dielectric constant and refractive index. On the other hand, on the basis of the crystal structure of bR

and classical electrostatics, effective values of the medium parameters are estimated for the retinal-binding pocket. By combining these results, we can successfully reproduce the opsin shifts of both bR<sub>568</sub> and M<sub>412</sub>. Next, the calculated opsin shift is decomposed into the contributions of the above four mechanisms. We will show that mechanism (4) plays a decisive role in the occurrence of the opsin shift. In addition, we will also refer to the spectral tuning mechanism in Rh.

## Theory

We briefly describe the SCRFP method used here (the details are described in ref 33). In this method, a solute molecule is embedded in a cavity made in an infinitely extended dielectric continuum. The charge distribution of the solute polarizes the dielectric, so that the reaction field is generated which acts back on the solute molecule. The Hamiltonian  $\hat{H}$  of the solute is written by

$$\hat{H} = \hat{H}_0 + V \quad (1)$$

where  $\hat{H}_0$  is the Hamiltonian of the solute molecule *in vacuo* and  $V$  is the perturbation term representing the effect of the reaction field. The electronic state of the solute molecule is determined by solving the following Schrödinger equation

$$\hat{H}|\Psi\rangle = E|\Psi\rangle \quad (2)$$

If we focus on the ground state  $\Psi_0$ , the Helmholtz energy is given by

$$\begin{aligned} A_0 &= \langle \Psi_0 | \hat{H}_0 | \Psi_0 \rangle + \frac{1}{2} \langle \Psi_0 | V | \Psi_0 \rangle \\ &= E_0 + \frac{1}{2} \{ \mathbf{P}_0 \mathbf{T}_{\text{stat}} \mathbf{P}_0 + \mathbf{P}_0 \mathbf{J}_{1\text{stat}} + \\ &\quad \mathbf{J}_{2\text{stat}} \mathbf{P}_0 + \mathbf{B}_{\text{stat}} \} \quad (3) \end{aligned}$$

where  $E_0$  and  $\mathbf{P}_0$  are the energy and electron density matrix of the solute molecule in the ground state, respectively.  $\mathbf{T}_{\text{stat}}$ ,  $\mathbf{J}_{1\text{stat}}$ ,  $\mathbf{J}_{2\text{stat}}$ , and  $\mathbf{B}_{\text{stat}}$  are matrixes whose elements depend only on the geometry of the solute, the dielectric constant of the medium, and the shape of the cavity. The subscript “stat” indicates that the matrix is a function of the static dielectric constant  $\epsilon_{\text{stat}}$ . The matrix  $\mathbf{T}_{\text{stat}}$  plays a role in mediating the interaction between the initial electronic distribution of the solute molecule and the reaction field originated in itself. The roles of  $\mathbf{J}_{1\text{stat}}$ ,  $\mathbf{J}_{2\text{stat}}$ , and  $\mathbf{B}_{\text{stat}}$  can be interpreted in a similar way: interactions between nuclei–electrons, electrons–nuclei, and nuclei–nuclei, respectively.<sup>34</sup>

Upon excitation, the induced dipole of the solvent molecule relaxes according to the change in electronic distribution of the solute molecule, while the orientational dipole is frozen as it is in the ground state. The relaxation of induced dipole arises from electronic polarization, which is closely related to the optical (high-frequency limit) dielectric constant  $\epsilon_{\text{opt}}$ . ( $\epsilon_{\text{opt}}$  is nearly equal to the square of the refractive index  $n$ .) In actual solvents,  $\epsilon_{\text{stat}}$  involves both contributions of orientational and electronic polarizations, and thereby their relaxation behavior should be expressed by correcting the effect of  $\epsilon_{\text{stat}}$  for that of  $\epsilon_{\text{opt}}$ . The final expression for the excitation energy  $\Delta A_i$  in solution is given by

$$\begin{aligned} \Delta A_i &= E_i - E_0 + \frac{1}{2} \{ (\mathbf{P}_i - \mathbf{P}_0) \mathbf{T}_{\text{stat}} \mathbf{P}_0 + (\mathbf{P}_i - \mathbf{P}_0) \mathbf{J}_{1\text{stat}} + \\ &\quad \mathbf{P}_i \mathbf{T}_{\text{opt}} (\mathbf{P}_i - \mathbf{P}_0) + \mathbf{J}_{2\text{opt}} (\mathbf{P}_i - \mathbf{P}_0) \} \quad (4) \end{aligned}$$

where  $E_i$  and  $\mathbf{P}_i$  are the energy and electron density matrix of

(28) For example, (a) Muthukumar, M.; Weimann, L. *J. Chem. Phys. Lett.* **1978**, *53*, 436. (b) Kakitani, H.; Kakitani, T.; Rodman, H.; Honig, B. *Photochem. Photobiol.* **1985**, *41*, 471. (c) Beppu, Y.; Kakitani, T. *Photochem. Photobiol.* **1994**, *59*, 660. (d) Tallent, J. R.; Hyde, E. W.; Findsen, L. A.; Fox, G. C.; Birge, R. R. *J. Am. Chem. Soc.* **1992**, *114*, 1581. (e) Gilson, H. S. R.; Honig, B. H.; *J. Am. Chem. Soc.* **1988**, *110*, 1943.

(29) Han, M.; DeDecker, B. S.; Smith, S. O. *Biophys. J.* **1993**, *65*, 899.

(30) (a) Han, M.; Smith, S. O. *Biochemistry* **1995**, *34*, 1425. (b) Han, M.; Smith, S. O. *Biophys. Chem.* **1995**, *56*, 23.

(31) See for review: Tomasi, J.; Perisico, M. *Chem. Rev.* **1994**, *94*, 2027.

(32) (a) Raudino, A.; Zuccarello, F.; Buemi, G. *J. Chem. Soc., Faraday Trans. 2* **1983**, *79*, 1759. (b) Zuccarello, F.; Raudino, A.; Buemi, G. *J. Mol. Struct. (THEOCHEM)* **1984**, *107*, 215.

(33) Houjou, H.; Sakurai, M.; Inoue, Y. *J. Chem. Phys.* **1997**, *107*, 5652.

(34) (a) Hoshi, H.; Sakurai, M.; Inoue, Y.; Chûjô, R. *J. Chem. Phys.* **1987**, *87*, 1107. (b) Hoshi, H.; Sakurai, M.; Inoue, Y.; Chûjô, R. *J. Mol. Struct. (THEOCHEM)* **1988**, *180*, 267.

the solute molecule in the  $i$ th excited state, respectively. The subscript "opt" indicates that the matrix is a function of  $\epsilon_{\text{opt}}$ .

To obtain an approximate value of  $\Delta A_i$  in the framework of single excitation configuration interaction (CI), one needs to modify the elements of the CI matrix for the *in vacuo* state. For the excited configuration  $\Psi_i$  which is generated by the transition from an occupied orbital  $\psi_a$  to a virtual orbital  $\psi_r$ , one obtains the diagonal elements of the CI matrix as follows

$$\begin{aligned} \Delta A_i^{(0)} &= \langle \Psi_i | \hat{H}_0 | \Psi_i \rangle + \frac{1}{2} \langle \Psi_i | \hat{V} | \Psi_i \rangle - A_0 \\ &= \epsilon_r(\epsilon_{\text{stat}}) - \epsilon_a(\epsilon_{\text{stat}}) - J_{\text{ar}} + 2K_{\text{ar}} + \\ &\quad \frac{1}{2} \langle \Psi_i | \hat{V} | \Psi_i \rangle \quad (5) \end{aligned}$$

where  $\epsilon_a(\epsilon_{\text{stat}})$  is an orbital energy for  $\psi_a$  that depends on  $\epsilon_{\text{stat}}$  and  $J_{\text{ar}}$  and  $K_{\text{ar}}$  are the Coulomb and exchange integrals, respectively.  $\langle \Psi_i | \hat{V} | \Psi_i \rangle$  is a state-dependent perturbation term defined as

$$\langle \Psi_i | \hat{V} | \Psi_i \rangle = -J_{2\text{stat}}(\mathbf{P}_i - \mathbf{P}_0) - \mathbf{P}_0 \mathbf{T}_{\text{stat}}(\mathbf{P}_i - \mathbf{P}_0) + J_{2\text{opt}}(\mathbf{P}_i - \mathbf{P}_0) + \mathbf{P}_i \mathbf{T}_{\text{opt}}(\mathbf{P}_i - \mathbf{P}_0) \quad (6)$$

In analogy with eq 6, the off-diagonal elements  $\langle \Psi_i | \hat{V} | \Psi_j \rangle$  could be written by using the reaction field matrixes  $\mathbf{J}_2$  and  $\mathbf{T}$ .<sup>33</sup> Finally, diagonalization of the modified CI matrix gives a set of excitation energy.

The expression of the excitation energy including solvent effects (eq 4) apparently consists of three portions: the term related to the solute molecule alone and two correction terms related to  $\epsilon_{\text{stat}}$  and  $\epsilon_{\text{opt}}$ . The reaction field potential changes as a function of  $f(\epsilon)$ , where

$$f(\epsilon) = \frac{\epsilon - 1}{\epsilon + 1} \quad (7)$$

This means that the values of the matrix elements for  $\mathbf{J}_1$ ,  $\mathbf{J}_2$ , and  $\mathbf{T}$  are functions of  $f(\epsilon)$ .

Therefore, it is expected that the absorption maximum  $\nu_{\text{max}}$  (given in energy unit) of the solute approximately follows the two-dimensional linear equation depending on  $f(\epsilon_{\text{stat}})$  and  $f(\epsilon_{\text{opt}})$ :

$$\nu_{\text{max}} = Af(\epsilon_{\text{stat}}) + Bf(\epsilon_{\text{opt}}) + C \quad (8)$$

where the coefficients  $A$ ,  $B$ , and  $C$  are the parameters intrinsic to the given solute molecule, including its geometry and shape of the cavity.

## Calculations

**Modeling of Chromophores.** The structure of molecules examined here are shown in Figure 1: *all-trans-6s-cis-retinal* (**1**), *all-trans-6s-cis-retinylideneethylamine* (**2**), *all-trans-6s-cis-retinylideneethylammonium cation* (**3a**), *all-trans-6s-cis-retinylideneethylammonium acetate* (**3b**), *all-trans-6s-trans-retinylideneethylammonium cation* (**4a**), *all-trans-6s-trans-retinylideneethylammonium acetate* (**4b**), 13-*cis-6s-trans-retinylideneethylamine* (**5**), the model compounds of 11-*cis-6s-cis-retinylideneethylammonium acetate* (**6a-f**), 13,14-dihydro-*all-trans-6s-cis-retinal* (**7a**), 13,14-dihydro-*all-trans-6s-cis-retinylideneethylammonium cation* (**7b**), 13,14-dihydro-*all-trans-6s-trans-retinal* (**7c**), 13,14-dihydro-*all-trans-6s-trans-retinylideneethylammonium cation* (**7d**), 3,7,11-trimethyldodeca-4,6,8,10-tetraenol (**8a**), 3,7,11-trimethyldodeca-4,6,8,10-tetraenylideneethylammonium cation (**8b**), and 11-*cis-6s-cis-retinylideneethylammonium acetate* (**9**).

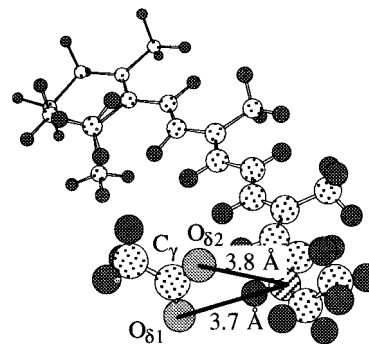


**Figure 2.** Molecular structure of the chromophore-counterion complex (**4b**) taken from the crystal structure of bR.<sup>20</sup>

For all the molecules except **4b**, the geometrical parameters were optimized with the PM3 method<sup>35</sup> packed in the MOPAC 6.0 program.<sup>36</sup> The resulting geometry of **3b** was as follows: the  $\text{O}_1\text{—C—O}_2$  plane of the acetate is almost contained in the conjugated plane of retinal, and the distances of  $\text{O}_1\text{—N}$ ,  $\text{O}_2\text{—N}$ , and  $\text{C—N}$  are 2.7, 3.4, and 3.5 Å, respectively ( $\text{O}_2$  is closer to C14). As for **4a** and **5**, the dihedral angle of  $\text{C}_5\text{—C}_6\text{—C}_7\text{—C}_8$  was fixed at  $180^\circ$ , while **1–3** have skewed *cis*-forms with respect to the  $\text{C}_6\text{—C}_7$  bond. **4b** is a model of the complex of the chromophore retinal including the side chains of Lys216 and Asp85 residues, and their atomic coordinates were taken from the crystal structure of bR<sup>20</sup> deposited with the Protein Data Bank<sup>48</sup> as 2BRD. Since the crystal structure lacks the coordinates of hydrogen atoms, we added hydrogen atoms by using LEaP module of the AMBER 4.1 program.<sup>37</sup> Figure 2 shows the structure of **4b**, where the  $\text{O}_{\delta 1}\text{—C}_\gamma\text{—O}_{\delta 2}$  plane of the acetate group is almost perpendicular to the conjugated plane

(35) Stewart, J. J. P. *J. Comput. Chem.* **1989**, *10*, 209.

(36) Stewart, J. J. P.; Frank, J. MOPAC Ver6.01; Seilar Research Laboratory, U. S. Air Force Academy: Colorado Springs, CO 80840-6528, 1989.

(37) Pearlman, D. A.; Case, D. A.; Caldwell, J. W.; Ross, W. S.; Cheatham III, T. E.; Ferguson, D. M.; Seibel, G. L.; ChandraSingh, U.; Weiner, P. K.; Kollman, P. A. AMBER ver. 4.1; University of California, San Francisco, 1995.

(38) (a) Krough-Jespersen, K.; Ratner, M. *J. Chem. Phys.* **1976**, *65*, 1305. We adopted the  $\beta^0$  value of  $-30$  eV for oxygen according to (b) Faure, P. J. J.; Chalvet, O.; Jaffe, H. H. *J. Phys. Chem.* **1981**, *85*, 473. (c) Rajzmann, M.; Francois, P. QCPE 11 **1979**, 382.

(39) Furuki, T.; Umeda, A.; Sakurai, M.; Inoue, Y.; Chūjō, R.; Harata, K. *J. Comput. Chem.* **1994**, *15*, 90.

(40) Inoue, Y.; Tokitō, Y.; Chūjō, R.; Miyoshi, Y. *J. Am. Chem. Soc.* **1977**, *99*, 5592.

(41) *Lange's Handbook of Chemistry*, 11th ed.; Dean, J. A. Ed.; McGraw-Hill: New York, 1973.

(42) The volume of the binding pocket defined in the text was calculated as follows: (i) calculate the surface area ( $S$ ) of the interlocking spheres whose radii are  $R = 5$  Å; (ii) calculate the surface area ( $s$ ) of the interlocking spheres whose radii are van der Waals radii ( $r$ ) of each atom; (iii) the volume of the region enclosed by these two interlocking spheres is estimated by  $(1/3)(RS - rs)$ .

(43) Bashold, B.; Gerwert, K. *J. Mol. Biol.* **1992**, *224*, 473.

(44) According to ref 43, the  $\text{pK}_a$  values of the ionizable residues in bR were consistently reproduced on the assumption that the dielectric constant of the protein interior was 4.0.

(45) Mogi, T.; Marti, T.; Khorana, H. G. *J. Biol. Chem.* **1989**, *264*, 14197.

(46) Hisatomi, O.; Kayada, S.; Aoki, Y.; Iwasa, T.; Tokunaga, F. *Vision Res.* **1994**, *34*, 3097.

(47) Nakayama, T.; Khorana, H. G. *J. Biol. Chem.* **1991**, *266*, 4269.

(48) (a) Abola, E. E.; Bernstein, F. C.; Koetzle, T. F.; Weng, J. Protein Data Bank. In *Crystallographic Databases-Information Content, Software Systems, Scientific Applications*; Allen, F. H., Bergerhoff, G., Siebers, R., Eds.; Data Commission of the International Union of Crystallography: Bonn/Cambridge/Chester, 1987; pp 107–132. (b) Bernstein, F. C.; Koetzle, T. F.; Williams, G. J. B.; Meyer, E. F., Jr.; Brice, M. D.; Rodgers, J. R.; Kennard, O.; Shimonouchi, T.; Tasumi, M. The Protein Data Bank: a Computer-based Archival File for Macromolecular Structures *J. Mol. Biol.* **1977**, *112*, 535.

of retinal, and the  $O_{\delta 1}-N$ ,  $O_{\delta 2}-N$ , and  $C_{\gamma}-N$  distances are 3.7, 3.8, and 4.0 Å, respectively.

**6b–f** are models of the chromophore of Rh. They are different from each other in spacial arrangement of the counterion. The procedure of constructing **6a–f** was as follows. First, the geometries of **6a** and the acetate ion were separately optimized. Then, the dihedral angles of C5–C6–C7–C8 and C11–C12–C13–C14 of **6a** were fixed at 45° and –140°, respectively.<sup>29</sup> Next, in **6b**, one of the oxygen atoms of the carboxylate was placed at a distance of 3.0 Å from C12 so as to make an angle  $O_1-C12-H12$  of 60°. Such an arrangement of the counterion is similar to that assumed in Smith's report.<sup>29</sup> In **6c**, the counterion is placed near C14 in a fashion similar to **6b**. In **6d**, the acetate is arranged so that  $O_1-H14-C14$  and  $O_2-H12-C12$  make straight lines, with keeping distances of  $O_1-C14$  and  $O_2-C12$  to be 3.0 Å. In **6e** and **6f**, the acetate ion was placed so that the  $O_1-C-O_2$  plane coincides with the conjugated plane of retinal and that  $N-H(N)-C(\text{carbonyl})$  makes a straight line. The distance between N and C(carbonyl) for **6e** and **6f** were 4.5 and 3.5 Å, respectively. For **9**, the retinal moiety was at first optimized, and then acetate anion was added in the same way as **6e**.

**Computational Details.** The computational scheme based on the SCRF method described in the section of theory was incorporated into the INDO/S molecular orbital program,<sup>38</sup> which can handle a single-excitation configuration interaction (CI). We took into account the configurations whose zeroth order excitation energies were lower than 10 eV. This threshold was confirmed to be sufficient in reproducing the experimental absorption maxima of retinal derivatives. For each molecule, the lowest  $\pi-\pi^*$  excitation energy was regarded as the calculated absorption maximum.

The medium surrounding a solute is characterized by two nonspecific parameters, i.e., static dielectric constant  $\epsilon$  and refractive index  $n$ . The calculations of electronic transitions were performed for several sets of  $\epsilon$  and  $n$  values. The values of  $\epsilon$  were taken to be 1.0, 2.0, 4.0, 8.0, and 40.0, and those of  $n$  were to be 1.0, 1.2, 1.4, and 1.6.

Basically, the cavity in which the solute molecule was accommodated was prepared according to the following previously reported procedure:<sup>39</sup> (1) a van der Waals sphere was placed at each atomic center of the solute molecule; (2) the surface of each sphere was divided into longitude-latitude grids with a dividing angle of 10°; (3) grid points placed in the overlapping region of the van der Waals spheres were deleted. The van der Waals radii used are equal to the sum of solute and solvent van der Waals radii (H: 2.77Å, C: 3.16Å, N: 3.07Å, O: 2.97Å). Unfortunately, we found that such a simple procedure often caused serious errors in the CI energies. This means that the accuracy of the excitation energy calculation more sensitively depends on the way of tessellation compared with that of the ground-state energy calculation. Here, we added some modifications to the above procedure, especially for the treatment of grids placed in the region where two van der Waals spheres are joining. The details of modification will be published elsewhere.

## Experimental Section

*All-trans*-retinal and *all-trans*-retinylidenebutylamine (abbreviated as *all-trans*-RSB) were prepared according to a procedure described elsewhere.<sup>40</sup> Each compound was dissolved in each of the 20 aprotic solvents listed in Table 1. Protonated *all-trans*-retinal Schiff base (abbreviated as *all-trans*-PRSB) was prepared by adding an excess amount of dichloroacetic acid to each solution of *all-trans*-RSB. All

**Table 1.** List of the Aprotic Solvents Used for UV–vis Measurements

no.	solvent	dielectric constant ( $\epsilon$ )	refractive index ( $n$ )
1	pentane	1.84	1.358
2	hexane	1.89	1.375
3	heptane	1.92	1.388
4	benzene	2.27	1.501
5	toluene	2.38	1.494
6	diethyl ether	4.34	1.350
7	diisopropyl ether	3.88	1.366
8	tetrahydrofrane	7.58	1.405
9	1,4-dioxane	2.21	1.420
10	ethyl acetate	6.02	1.373
11	acetone	20.7	1.359
12	2-butanone	18.5	1.376
13	dimethyl sulfoxide	45.8	1.477
14	acetonitrile	37.5	1.346
15	dimethylformamide	36.7	1.429
16	pyridine	12.3	1.523
17	carbontetrachloride	2.23	1.463
18	chloroform	4.81	1.446
19	dichloromethane	8.90	1.424
20	1,2-dichloroethane	10.4	1.442

photoactive compounds were handled in the dark. UV–vis spectra were recorded on a Shimadzu UV-2100 spectrometer at room temperature.

## Results

***all-trans*-Retinal and *all-trans*-RSB.** To assess the reliability of the SCRF method described above, we first compared the calculated results for **1** and **2** with the corresponding experimental data. As described in the section of theory, the excitation energy depends on the medium parameters,  $\epsilon_{\text{stat}}$  and  $\epsilon_{\text{opt}}$ , according to eq 8. Hereafter, the static dielectric constant  $\epsilon_{\text{stat}}$  is simply denoted as  $\epsilon$ , and the optical dielectric constant  $\epsilon_{\text{opt}}$  as  $n^2$ . Then, eq 8 is rewritten as follows

$$\nu_{\text{max}} = Af(\epsilon) + Bf(n^2) + C \quad (9)$$

In eq 9, coefficients  $A$  and  $B$  can be regarded as measures of sensitivity to  $\epsilon$  and  $n^2$ , respectively, while  $C$  is the extrapolated value of the excitation energy toward the *in vacuo* state. The first term involves both orientational and electronic polarization effects of solvents, while the second term does only the electronic effect. A way of assessing the accuracy of the calculation is to compare the values of these coefficients with the corresponding experimental values.

Figure 3 shows the absorption maxima of *all-trans*-retinal measured in various solvents. The horizontal axis indicates regression values, obtained from minimum square fitting against eq 9. The optimum values of  $A$ ,  $B$ , and  $C$  are summarized in Table 2. There is good correlation between the observed and regression values. Thus, the solvatochromic shift of *all-trans*-retinal is well explained in terms of the continuum model, if the electronic polarization effects of solvents are exactly taken into account. A few exceptions are, however, found for the results in chloroform and dichloromethane (solid circles), in which some specific interactions might work. These data points were excluded in the fitting calculation. The values of  $A$  and  $B$  are negative, indicating that the effects depending on  $\epsilon$  and  $n$  both cause red shifts. It should be noted that the absolute value of  $B$  is considerably larger than that of  $A$ , indicating that the effect of electronic polarization of solvent more strongly affects the absorption maxima of the solute than does that of orientational polarization.

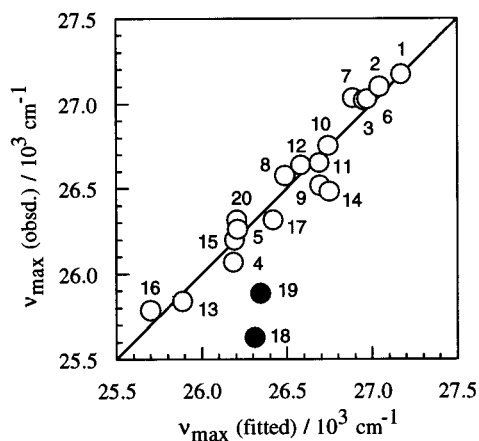


**Figure 3.** Correlation between the observed absorption maxima of *all-trans*-retinal and their regression values based on eq 9. Numbers represent the solvents listed in Table 1. Solid symbols indicate the data excluded from the regression analysis.

**Table 2.** Comparison between Experimental and Calculated Results of Regression Analysis for the Absorption Maxima of *all-trans*-Retinal and *all-trans*-RSB

	coefficients <sup>a</sup> ( $10^3 \text{ cm}^{-1}$ )		
	A	B	C
<i>all-trans</i> -Retinal			
exptl	-0.78	-10.35	30.5
calcd	-0.46	-9.13	29.2
<i>all-trans</i> -RSB			
exptl <sup>b</sup>	-0.29	-8.75	30.8
calcd	-0.32	-4.68	29.7
13- <i>cis</i> -RSB			
calcd	-0.19	-8.12	27.8

<sup>a</sup> Based on eq 10. <sup>b</sup> Results for *all-trans*-retinylidenebutylamine.

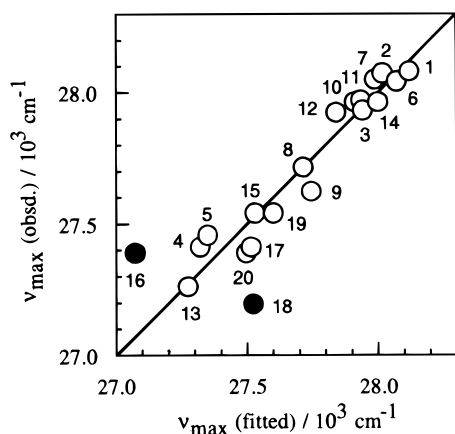


**Figure 4.** Correlation between the observed absorption maxima of *all-trans*-RSB and their regression values based on eq 9. Numbers represent the solvents listed in Table 1. Solid symbols indicate the data excluded from the regression analysis.

The results for *all-trans*-RSB are shown in Figure 4 and also in Table 2. As shown in Figure 4, the experimental absorption maxima are in good agreement with their regression values. Thus, the solvatochromic shift of *all-trans*-RSB can be also described by the continuum approximation. There are also a few exceptions for the results in chloroform and pyridine. Table 2 shows that the  $\epsilon$ - and  $n^2$ -dependent shifts of the absorption maximum of RSB occurs in a way similar to those for retinal, although the absolute values of the coefficients *A* and *B* are smaller.

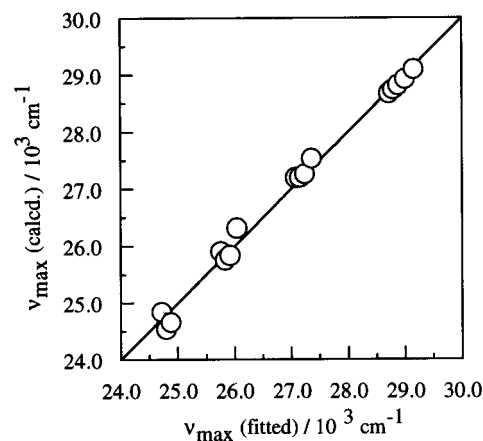


**Figure 5.** Correlation between the calculated absorption maxima of *all-trans*-retinal and their regression values based on eq 9.

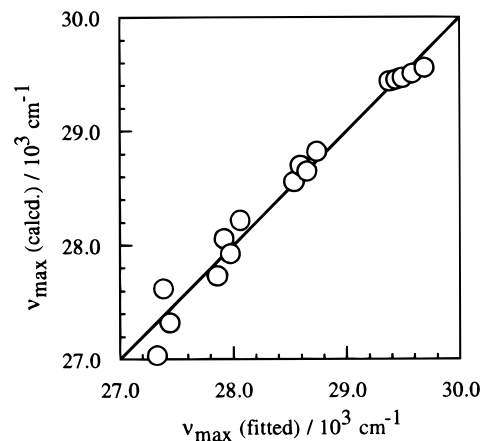


**Figure 6.** Correlation between the calculated absorption maxima of *all-trans*-RSB and their regression values based on eq 9.

Regression analysis is also necessary for processing primary data from the calculation because usually these are scattering due to numerical errors occurring in the solvent effect calculation, especially in the numerical evaluation of the reaction field. In addition, the determination of the coefficients *A*, *B*, and *C* allows one to obtain the theoretical value for an arbitrary set of ( $\epsilon$ ,  $n$ ). Figures 5 and 6 show the results of regression analysis. As similar to the case of experiments, the calculated values of the absorption maxima for **1** and **2** are well fitted to eq 9. The results from the calculations summarized in Table 2 fairly coincide with those from the experiment, which ensures us of the reliability of the present SCRF-CI method. For the sake of the subsequent discussion, in Table 2 the calculated results for 13-*cis*-RSB (**5**) are also listed.

**Protonated Schiff Bases.** In contrast to the cases of retinal and RSB, there are apparent deviations from eq 9 in most of the *all-trans*-PRSB solutions studied here. This may imply the occurrence of specific interactions between the solute and solvent. As reported by Blatz et al.,<sup>17</sup> polar solvents such as alcohol and ether form hydrogen bond complexes with PRSB and hence they shield the electrostatic effect of a counterion. It is known as “leveling effect”. The fitting calculation was thus performed for solutions of nonpolar and nonbasic solvents, 1–5 and 17. The resulting coefficients *A*, *B*, and *C* are summarized in Table 3. As shown in Figure 7, the absorption maxima observed for all the polar and basic solvents (solid circles) are blue shifted in comparison with the values predicted from the regression equation. We do not make further analysis of them,

**Table 3.** Results of Regression Analysis for the Absorption Maxima of *all-trans*-PRSBs

	coefficients <sup>a</sup> ( $10^3 \text{ cm}^{-1}$ )		
	A	B	C
exptl <sup>b</sup>	-3.47	-3.57	24.6
<b>3a</b>	0.41	-2.90	20.9
<b>3b</b>	-0.09	-5.53	24.8
<b>4a</b>	0.50	-3.02	18.8
<b>4b</b>	-0.23	-6.58	21.1

<sup>a</sup> Based on eq 10. <sup>b</sup> Results for *all-trans*-retinylidenebutylammonium dichloroacetate.

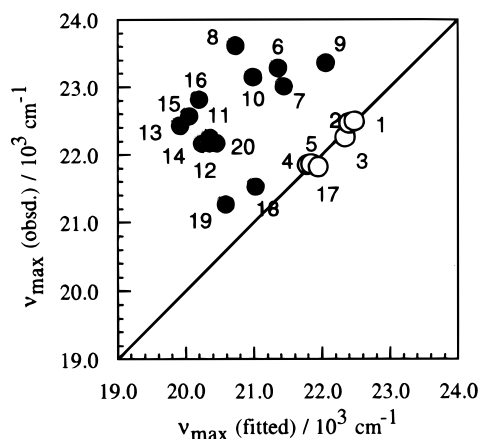


**Figure 7.** Correlation between the observed absorption maxima of *all-trans*-PRSB and their regression values based on eq 9. Numbers represent the solvents listed in Table 1. Solid symbols indicate the data excluded from the regression analysis.

because our main interest is to extract the solvatochromic shifts following the linear response theory described in the section of theory.

The calculation was carried out for two types of PRSB: *all-trans*-6*s-cis*-retinylideneethylammonium cation (**3a**) and *all-trans*-6*s-cis*-retinylideneethylammonium acetate (**3b**) (for detail, see the calculation section). The results are summarized in Table 3. The value of *A* for **3a** is positive, suggesting that a blue shift occurs with an increase in  $\epsilon$ , while that for **3b** is negative. In both cases, the absorption maxima are less sensitive to the static dielectric constant  $\epsilon$ . The values of coefficient *B* for **3a** and **3b** both are relatively large negative values, indicating that a significant amount of red shift is induced with an increase in  $n$ . In addition, the *B* value of **3b** is about twice larger than that of **3a**. The origin of the difference in the *A* and *B* values between **3a** and **3b** is discussed later in the section of "Cooperative action between counterion effect and polarizable medium effect".

Table 3 also lists the values of coefficients *A*, *B*, and *C* for the solvatochromic shifts of **4a** and **4b**, both of which have 6*s-trans* conformation about the C6–C7 bond. The *A* value for the cationic species (**4a**) is positive, whereas that for a PRSB salt (**4b**) is negative. The *B* values for **4a** and **4b** both are negative, but the latter is about twice larger than the former. These relationships are quite similar to those found for **3a** and **3b**, indicating that the tendency of the solvatochromic shift is hardly influenced by the change of the ring/chain conformation.

*all-trans*-PRSB has 6*s-cis* conformation about the C6–C7 bond in solution.<sup>5</sup> In this regards, **3b** is a better model for the solution state of PRSB than **4b**. There is a considerable difference in the *A* value between the experimental and calculated results. In comparison with the results for retinal and RSB, the experimental *A* value for PRSB is extremely large,

indicating the less accuracy of the data for PRSB. Namely, the experimental values may be less reliable, since the regression analysis was performed with insufficient number of data points. The calculated *B* value for **3b** is  $-5.53 \times 10^3 \text{ cm}^{-1}$ , while the experimentally obtained *B* value for *all-trans*-PRSB is  $-3.57 \times 10^3 \text{ cm}^{-1}$ . In this case, the calculated results moderately encouraging. However, to check the reliability of the calculations, further assessment would be needed.

The calculated values were compared with the results reported by Kliger et al.,<sup>25a</sup> who measured the absorption maxima of PRSB in phenol/ethanol solution. According to their results, the amount of red shift ( $\Delta\nu$ ) of absorption maxima is in proportion to the concentration of phenol

$$\Delta\nu = k[\text{phenol}] \quad (10)$$

where *k* is a constant and [phenol] is the concentration of phenol. In addition, it was interpreted that such a red-shift arises from the increase in polarizability of solvent with an increase in phenol concentration. The polarizability of solvent was given by

$$\alpha = \frac{3M}{4\pi N_a d} \left( \frac{n^2 - 1}{n^2 + 1} \right) \quad (11)$$

where  $N_a$  is Avogadro's number and  $\alpha$ , *M* and *d* are the polarizability ( $11.0 \times 10^{-24} \text{ cm}^3$ ), molecular weight and density of phenol, respectively. From eqs 7, 10 and 11, we can obtain the following relationship between the amount of red shift and refractive index *n*.

$$\Delta\nu = k \left( \frac{3}{4\pi N_a \alpha} \right) f(n^2) \quad (12)$$

Comparing eq 12 with eq 9, we can see that the factor  $k(3/4\pi N_a \alpha)$  corresponds to the coefficient *B*. From Figure 1 of ref 13a, *k* is estimated to be  $234 \text{ cm}^{-1} \text{ M}^{-1}$ . The *B* value can be estimated to be  $-6.5 \times 10^3 \text{ cm}^{-1}$ , which is very close to our calculated result. Therefore, it is expected that the present calculation can accurately predict the solvatochromic shifts of PRSB as well as those of retinal and RSB.

**Details of the Counterion Effect.** As already described, the *C* value corresponds to the absorption maxima *in vacuo*. Quite naturally, the *C* values obtained by this procedure well agree with the absorption maxima obtained from *in vacuo* SCF–CI calculations (data not shown). The difference in the *C* values between **3b** and **4b** is  $3.7 \times 10^3 \text{ cm}^{-1}$ . This difference may arise from two geometrical factors: difference in the location of counterion and difference in the conformation about the C6–C7 bond.

To investigate which factor is responsible for such a spectral difference, we calculated the absorption maxima for **3b** and **4b** with changing the location of the counterion. A unit negative charge was placed on the extended line of the N–H bond of PRSB, instead of explicitly treating the counterion (these models are denoted as **3b'** and **4b'**). According to an early work by Blatz et al.,<sup>8b</sup> the absorption maximum of PRSB red shifts with increasing size of the counterion, namely in the order of  $\text{I}^- > \text{Br}^- > \text{Cl}^-$ . And they indicated that the amount of red shift is nearly proportional to  $1/d^2$ . Here we also apply a similar analysis to the calculated data for **3b'** and **4b'**.

In Figure 8 are the absorption maxima (filled symbols) of **3b'** and **4b'** plotted against  $1/d^2$ , where *d* is the distance between the *N* atom and the charge. The absorption maxima are certainly proportional to  $1/d^2$  and the slopes ( $\Delta C_{\text{counterion}}$ ) for **3b'** and **4b'**

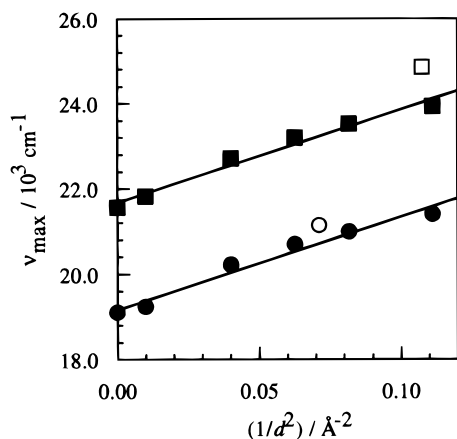


**Figure 8.** Calculated absorption maxima of 6*s*-*cis*-all-*trans*-PRSB (■) and 6*s*-*trans*-all-*trans*-PRSB (●) as a function of  $1/d^2$ , where  $d$  is the distance between the Schiff base nitrogen and a negative point charge. The absorption maxima of **3b** (□) and **4b** (○) are superposed.

are nearly equal to each other ( $21.9 \times$  and  $21.7 \times 10^3 \text{ cm}^{-1} \text{ \AA}^2$ , respectively). These findings indicate that the  $d$ -dependence of the absorption maxima is hardly affected with the C6–C7 conformation. Figure 8 also shows the plots of the absorption maxima (open symbols) of **3b** and **4b** against  $1/d^2$ , where  $d$  is the average value of the distance O<sub>1</sub>–N and O<sub>2</sub>–N ( $d_{3b} = 3.1 \text{ \AA}$  for **3b**, and  $d_{4b} = 3.8 \text{ \AA}$  for **4b**). As can be seen, the data points for **3b** and **4b** are almost placed on the regression lines for **3b'** and **4b'**, respectively. This indicates that the blue-shift induced on going from **3a** (**4a**) to **3b** (**4b**) is dominated by the electrostatic interaction between PRSB and its counterion. In Figure 8, the intercepts of the lines for **3b'** and **4b'** are distant by  $2.5 \times 10^3 \text{ cm}^{-1}$  (denoted as  $\Delta C_{C6-C7}$ ), which should correspond only to the contribution of the C6–C7 conformation change. This value almost agrees with the difference in the  $C$  value between **3a** and **4a** ( $2.1 \times 10^3 \text{ cm}^{-1}$ ). These facts indicate that additivity is held between the shift induced by the counterion and that induced by a conformational change about the C6–C7 bond. Consequently, we can summarize the relation between the *in vacuo* absorption maxima of **3b** ( $C_{3b}$ ) and **4b** ( $C_{4b}$ ) as follows

$$C_{4b} \cong C_{3b} - \left( \frac{1}{(d_{4b})^2} - \frac{1}{(d_{3b})^2} \right) \times \Delta C_{\text{counterion}} - \Delta C_{C6-C7} \quad (13)$$

where the second term originates from the difference in location of the counterion and the third term from the ring/chain coplanarization. They contribute to red shifts of  $1.2 \times 10^3$  and  $2.5 \times 10^3 \text{ cm}^{-1}$ , respectively.

Using **6a–f**, we investigated the dependence of the absorption maxima of PRSB on the spatial arrangement and orientation of a counterion. Figure 9(a) shows the calculated absorption maxima of **6a–f** as a function of  $f(n^2)$  ( $\epsilon$  was fixed to be four). When  $f(n^2) = 0.0$  ( $n = 1.0$ ), the absorption maxima of **6a–f** are ranging from  $19 \times$  to  $23 \times 10^3 \text{ cm}^{-1}$ . With an increase in  $n$ , the absorption maxima of **6a–e** appears to converge, but the data for **6f** keeps away from the others. Next, for each  $n$ , the data are plotted against  $1/d^2$ , where  $d$  is the average value of the distances O<sub>1</sub>–N and O<sub>2</sub>–N (Figure 9(b)). The curves in this figure are drawn after the treatment of quadratic regression for each set of the data. When  $n = 1.0$ , the absorption maxima almost change in proportion to  $1/d^2$ . This implies that the distance between PRSB and the counterion is the most important geometrical factor governing change of the absorption maxima

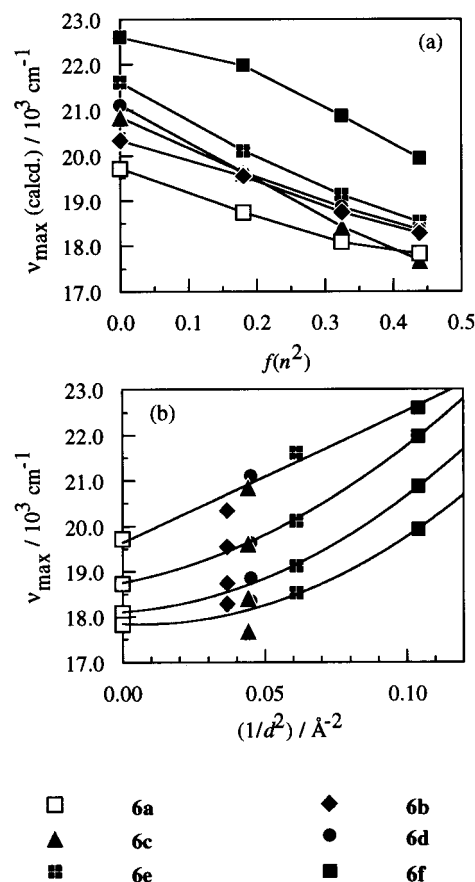


**Figure 9.** Absorption maxima of **6a–f** calculated under the condition of  $\epsilon = 4.0$ . (a) The data are plotted as a function of  $f(n^2)$ . (b) The data are plotted as a function of  $1/d^2$ , where  $d$  is the average value of the distances between the Schiff base nitrogen and the oxygen atoms of carboxylate.

and that the effects of the orientation and arrangement of the counterion are less important. With an increase in  $n$ , the absorption maxima red shift, and the contribution of the quadratic component becomes remarkable. As a consequence, when  $n$  is 1.6, the difference in the absorption maxima among **6a–e** is very small compared to the case of  $n = 1.0$ .

## Discussion

**The Opsin Shift of Bacteriorhodopsin.** The present calculations showed that the absorption maxima of PRSBs are significantly red shifted with an increase in the polarizability of solvent. This suggests the possibility that the major part of the opsin shift in bR is caused by the electronic polarization effect of the protein matrix. On the basis of the crystal structure of bR,<sup>20</sup> we can identify the amino acid residues around the chromophore. Here, the chromophore-binding pocket is defined as a region made by interlocking spheres, with a radius of  $5 \text{ \AA}$ , centered on each atom of the chromophore. In this region, we found seven aromatic residues: Tyr83, Trp86, Trp138, Trp182, Tyr185, Trp189, and Phe208 (Figure 10). The ratio of the number of these aromatic residues to that of the other residues in this region was 41%, in contrast to the ratio of only 14% for the whole protein. The assembly of these aromatic residues may act as a dielectric medium with a high refractive index. The effective refractive index of the binding pocket can be estimated with the aid of a theory of electrostatics. In general, the averaged refractive index for a mixed solvent can be

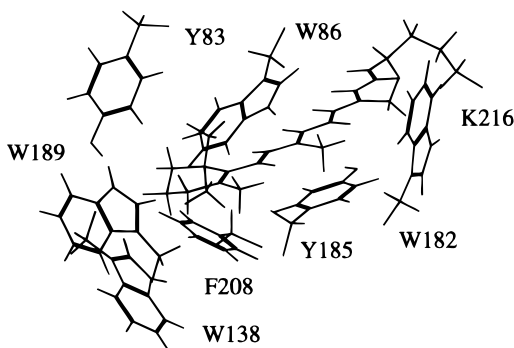


**Figure 10.** The molecular structure of the chromophore and the aromatic residues present within the chromophore-binding pocket. The coordinates of the heavy atoms were taken from the crystal structure<sup>20</sup> deposited with the Protein Data Bank.<sup>48</sup> Hydrogen atoms were added in the way as described in the section of “Modeling of Chromophores”.

**Table 4.** Polarizability and Density of Some Aromatic Compounds

	polarizability $4\pi\alpha/10^{-24}$ cm <sup>3</sup>	density <sup>a</sup> $\rho/g$ cm <sup>-3</sup>
benzene <sup>b</sup>	131.1	0.10
phenol <sup>c</sup>	138.7	0.24
indole <sup>d</sup>	187.2	0.60

<sup>a</sup> Density in the region of 5 Å-vicinity of the chromophore (see text).

<sup>b</sup> A model of the side chain of Phe. <sup>c</sup> A model of the side chain of Tyr.

<sup>d</sup> A model of the side chain of Trp.

estimated using the modified Lorentz–Lorenz equation given by

$$\frac{n^2 - 1}{n^2 + 2} = \frac{4\pi N_a}{3} \sum_i \frac{\rho_i \alpha_i}{M_i} \quad (14)$$

where  $\rho_i$ ,  $\alpha_i$ , and  $M_i$  are density (given in g cm<sup>-3</sup>), polarizability, and molecular weight of the component  $i$ . Table 4 lists the polarizabilities of benzene, phenol, and indole, which were calculated from the data for atomic contribution to molar refraction.<sup>41</sup> By utilizing our program, which can be used to evaluate the surface area of a molecular cavity,<sup>42</sup> the volume of the chromophore-binding pocket was estimated to be 1300 Å<sup>3</sup>. In this region, there are four Trp side chains (indole), two Tyr side chains (phenol), and one Phe side chain (benzene). Consequently, the densities of indole, phenol, and benzene moieties are given by 0.60, 0.24, and 0.10 g cm<sup>-3</sup>, respectively (Table 4). The average refractive index for the chromophore-binding pocket is thus determined to be 1.51.

To define the opsin shift  $\Delta\nu$ , we adopt the absorption maximum of *all-trans*-PRSB in hexane as a reference. Namely,  $\Delta\nu = \nu_{\text{in hexane}} - \nu_{\text{in protein}}$ . As described in the section of “Results”, the absorption maxima of PRSB are interpreted in terms of the continuum model only when nonpolar and nonbasic solvents are used. In view of this, it is reasonable to choose hexane as the reference rather than methanol, which was often used in the previous studies.<sup>9</sup> Using the observed values of  $17.6 \times 10^3$  cm<sup>-1</sup> for bR<sub>568</sub> and  $22.5 \times 10^3$  cm<sup>-1</sup> for the reference, we can obtain  $4.9 \times 10^3$  cm<sup>-1</sup> as the opsin shift (Table 5). For theoretical evaluation of the opsin shift, **3b** was used as a model of *all-trans*-PRSB and **4b** as a model of the bR chromophore. The calculated absorption maxima of **3b** and **4b** are summarized in Table 5. The absorption maxima ( $23.1 \times 10^3$  cm<sup>-1</sup>) for **3b** in hexane was obtained by substituting the values of the coefficients  $A$ ,  $B$ , and  $C$  (given in Table 3) and the medium parameters for hexane ( $\epsilon = 1.89$ ,  $n = 1.375$ ) into eq 9. For **4b**, we used the value of 1.51 as the refractive index of bR, as

**Table 5.** Comparison between Experimental and Calculated Opsin Shifts for bR<sub>568</sub>, M<sub>412</sub>, and Rh<sub>500</sub>

	$\nu_{\text{max}}$ in hexane (10 <sup>3</sup> cm <sup>-1</sup> )	$\nu_{\text{max}}$ in protein (10 <sup>3</sup> cm <sup>-1</sup> )	opsin shift $\Delta\nu$ (10 <sup>3</sup> cm <sup>-1</sup> )
		bR <sub>568</sub>	
exptl	22.5	17.6	4.9
calcd	23.1	18.4	4.7
		M <sub>412</sub>	
exptl	28.1	24.3	3.8
calcd	28.2	24.5	3.7
		Rh <sub>500</sub>	
exptl	22.5	20.0	2.5
calcd	23.1	20.5	2.6

obtained above. Here the value of  $\epsilon$  was taken to be 4.0, according to recent studies using the Poisson–Boltzmann electrostatics.<sup>43,44</sup> Then, the absorption maximum of **4b** in the bR-mimic environment is evaluated to be  $18.4 \times 10^3$  cm<sup>-1</sup>. As a consequence, the opsin shift is evaluated to be  $4.7 \times 10^3$  cm<sup>-1</sup>, in excellent agreement with the observed value.

Similarly, we also analyzed the spectral shift observed for M<sub>412</sub>. The chromophore of M<sub>412</sub> is unprotonated 13-*cis* retinal Schiff base. The absorption maxima of *all-trans*-RSB in hexane was taken as a reference. Then, the observed opsin shift for M<sub>412</sub> is  $3.8 \times 10^3$  cm<sup>-1</sup>. In calculation, **2** was used as a model of *all-trans*-RSB and **5** as a model of the chromophore of M<sub>412</sub>. As shown in Table 5, the calculated absorption maxima of **2** and **5** are  $28.2 \times 10^3$  and  $24.5 \times 10^3$  cm<sup>-1</sup>, respectively. The resulting opsin shift is  $3.7 \times 10^3$  cm<sup>-1</sup>, again in excellent agreement with the observed value.

In summary, the opsin shifts of both bR<sub>568</sub> and M<sub>412</sub> can be explained by explicitly taking into account the polarizable medium effect of the aromatic residues surrounding the chromophore. It is known that most of the aromatic residues appearing in the retinal-binding pocket of bR are conserved across many retinal-bound proteins.<sup>45</sup> For example, Phe261, Trp265, and Tyr269 in bovine rhodopsin correspond to Trp182, Tyr185, and Trp189 in bR, respectively.<sup>46</sup> In fact, site-directed mutagenesis studies have shown that the replacement of these residues causes a significant amount of blue shift in both of bR and Rh.<sup>45,47</sup> For example, in the W182F mutant of bR the main absorption band appears at 491 nm. Now we attempt to calculate the opsin shift for Rh. For this purpose, compound **9** was selected as a model of the chromophore in Rh. Since there is no available data for the tertiary structure of Rh, the values of the medium parameters were assumed to be the same as determined for bR, namely  $\epsilon = 4.0$ ,  $n = 1.51$ . The results are summarized in Table 5. As expected, the calculated opsin shift ( $2.6 \times 10^3$  cm<sup>-1</sup>) is in good agreement with the observed value ( $2.5 \times 10^3$  cm<sup>-1</sup>). The above results strongly suggest that the polarizable medium effect, mechanism (4), is a common origin of the opsin shifts observed for retinal proteins.

**Decomposition of the Opsin Shift.** We can decompose the calculated opsin shift of bR<sub>568</sub> ( $4.7 \times 10^3$  cm<sup>-1</sup>) into at least three kinds of contributions (Table 6). The first is the effect of 6-*s-cis* → 6-*s-trans* conformational change (mechanism (1)), and the second is the weakening of the interaction of PRSB with its counterion in bR (mechanism (2)). These have already been estimated in the derivation of eq 13: namely, mechanisms (1) and (2) cause red shifts of  $2.5 \times 10^3$  and  $1.2 \times 10^3$  cm<sup>-1</sup>, respectively. Then, the residual shift is  $1.0 \times 10^3$  cm<sup>-1</sup>, which should be attributed to the polarizable medium effect of the protein (mechanism (4)). In what follows, we will compare these results with available experimental data.

**Table 6.** Results for Decomposition of the Opsin Shift<sup>a</sup>

	mechanism				(1)+(2) <sup>b</sup>	total
	(1) ring/chain	(2) counterion	(3) point charge	(4) medium		
this work	2.5	1.2		1.0		4.7
Hu et al. <sup>c</sup>	~2	~2	0	0	~1	~5
Yan et al. <sup>d</sup>	2.0		(2.1) <sup>e</sup>	(2.1) <sup>e</sup>		4.1

<sup>a</sup> Each contribution is given in  $10^3 \text{ cm}^{-1}$ . <sup>b</sup> Concerted effect of mechanisms (1) and (2). <sup>c</sup> Taken from ref 27. <sup>d</sup> Taken from ref 26. <sup>e</sup> The total contributions from mechanisms (3) and (4) is  $2.1 \times 10^3 \text{ cm}^{-1}$ .

**Table 7.** Calculated and Observed Absorption Maxima of 13,14-Dihydro-Retinal and Its Analogues<sup>a</sup>

	in methanol ( $\epsilon = 33, n = 1.327$ )		in protein ( $\epsilon = 4, n = 1.51$ )		opsin shift <sup>b</sup>	
	calcd	exptl <sup>c</sup>	calcd	exptl <sup>c</sup>	calcd	exptl <sup>c</sup>
	<b>7a</b>	36.8	34.6	35.5		
<b>7b</b>	35.4		35.3			
<b>7c</b>	32.3		32.3			
<b>7d</b>	32.1		31.9	30.5	4.9	4.1
<b>8a</b>	32.1	32.6	32.0			
<b>8b</b>	31.4		30.7	31.2	1.4	1.4

<sup>a</sup> Given in  $10^3 \text{ cm}^{-1}$ . <sup>b</sup> Obtained by subtracting the absorption maxima of the chromophore (**7d** and **8b**) in protein from those of the corresponding aldehyde (**7a** and **8a**) in methanol. <sup>c</sup> Taken from ref 26.

Hu et al.<sup>27</sup> pointed out the importance of cooperative effect of mechanisms (1) and (2). According to their experimental results, the former causes a red shift of  $\sim 2 \times 10^3 \text{ cm}^{-1}$  and the latter also does that of  $\sim 2 \times 10^3 \text{ cm}^{-1}$  (Table 6). A unique point of their hypothesis is that the combined action of (1) and (2) generates an additional red shift of  $\sim 1 \times 10^3 \text{ cm}^{-1}$ . However, according to our results (Figure 8), such a phenomenon is not observed. In Hu's experiments, butylamine Schiff base was used as *6s-cis*-PRSB, while aniline Schiff base as *6s-trans*-PRSB. Generally speaking, the use of models with different imine structures may suffer from a potential disadvantage in investigating the spectral tuning mechanism, because the absorption maximum of PRSB is very sensitive to a subtle difference in the Schiff base-counterion distance. Due to more bulkiness of the aniline group, the distance might be longer in the aniline Schiff base than in the butylamine Schiff base. If so, their observed data could be interpreted without considering a synergy between the two effects.

13,14-Dihydro-retinal (**7a**) is a better probe capable of escaping from the counterion effects, because its conjugated system is not linked to the Schiff base linkage. Considering this fact, Yan et al.<sup>26</sup> evaluated the opsin shifts for **7a** and its analogue (**8a**) as the change in absorption maximum on going from **7a** (or **8a**) in methanol to that in bR. Namely, in the reference state the chromophore is aldehyde, not Schiff base: this point is different from the conventional definition of the opsin shift. As shown in Table 7, the resulting opsin shifts for **7a** and **8a** were 4.1 and  $1.4 \times 10^3 \text{ cm}^{-1}$ , respectively. Our calculated results, following Yan's definition, are  $4.9 \times$  and  $1.4 \times 10^3 \text{ cm}^{-1}$  for **7a** and **8a**, respectively, in good agreement with the observed values.

**8a** has *s-trans* conformation about the C6–C7 bond because of lack of ionone ring, and thereby mechanism (1) does not operate on binding to the protein. In addition, the absence of such a bulky group has an advantage that there would be no significant steric interaction between the chromophore and the protein in the binding state. As a result, the opsin shift for **8a** is expected to more purely reflect the polarizable effect of the protein matrix than that for **7a**. This seems to be the main

reason the calculated value is in better agreement with the experimental value of **8a** than with that of **7a**. However, it should be noted that the opsin shift for **8a** involves not only the effect of the protein matrix but also the effect of the terminal structure on the Schiff base side, even if the terminal C=N double bond is not linked directly to the conjugated system. To examine the latter effect, we calculated the absorption maximum of **8b** in the methanol-like environment, namely  $\epsilon = 32.7$  and  $n = 1.327$ . As shown in Table 7, the structural conversion, on going from aldehyde to Schiff base, causes a red shift of  $0.7 \times 10^3 \text{ cm}^{-1}$ . Thus, the net contribution of the protein matrix occupying in the opsin shift for **8a** is estimated to be about  $0.7 \times 10^3 \text{ cm}^{-1}$ . This value is somewhat smaller than the value ( $1.0 \times 10^3 \text{ cm}^{-1}$ ) previously obtained from the analysis of the opsin shift for the native pigment. This is quite a reasonable result, considering the symmetric nature of the conjugated system of **8a**. Namely, unlike PRSB, the conjugated system of **8a** has no apparent dipole moment in the excited state, where an excessive stabilization would not be induced by interaction with solvent. Thus, the use of **7a** or **8a** tends to underestimate the polarizable effect of the protein matrix.

The calculated opsin shift for **7a** is larger than that for **8a** by  $3.5 \times 10^3 \text{ cm}^{-1}$ . It is reasonable to say that the major part of this difference arises from the coplanarization effect (mechanism (1)). In fact, the *6s-cis*  $\rightarrow$  *trans* conversion from **7b** to **7d** causes a red shift of  $3.3 \times 10^3 \text{ cm}^{-1}$ . On the other hand, the difference in the observed opsin shift between **7a** and **8a** is  $2.7 \times 10^3 \text{ cm}^{-1}$ , which is somewhat smaller than the calculated value. The difference between the calculated and observed values would be chiefly due to the occurrence in a steric interaction between **7a** and the protein. The analysis of such a phenomenon is beyond the scope of the present study.

The difference in the observed absorption maxima between **7a** and **8a** is  $2.0 \times 10^3 \text{ cm}^{-1}$  in methanol, a value which corresponds to the contribution of the ring/chain coplanarization. By subtracting this contribution from the total opsin shift for **7a** ( $4.1 \times 10^3 \text{ cm}^{-1}$ ), Yan et al. concluded that the net contribution of the protein environment was a red shift of  $2.1 \times 10^3 \text{ cm}^{-1}$ . This value is significantly larger than the above result ( $1.4 \times 10^3 \text{ cm}^{-1}$ ) deduced from the opsin shift for **8a**. For more complete argument against such a difference, it is necessary to obtain experimental data for the absorption maxima of **7b–7d** and **8b** and for the steric effect mentioned above.

In summary, the polarizable effect of the protein matrix actually works for the spectral tuning of bR. Its contribution is not less than  $1.0 \times 10^3 \text{ cm}^{-1}$  for the native chromophore.

**Cooperative Action between Counterion Effect and Polarizable Medium Effect.** As far as the protein matrix works as a polarizable medium, the opsin shift is reproducible even when an external charge is absent. This is understood from the possibility that the medium behaves like a counterion or an external charge. In the ground state, the positive charge of PRSB is localized on the  $-\text{CH}=\text{NH}-$  moiety, and hence the medium polarizes so as to maximally stabilize such a distribution of positive charge. In other words, solvent molecules cooperatively behaves like a counterion of PRSB. Upon excitation, the positive charge of PRSB is delocalized toward the  $\beta$ -ionone ring,<sup>23</sup> immediately followed by the electronic part of polarization of the medium. Then, the polarizable medium acts as if it were a mobile counterion. The result from such an action is similar to that expected for the external charge proposed by Nakanishi et al.<sup>12</sup>

To provide a rigid physical basis for the above interpretation, we examined the dependence of the energy levels of the ground

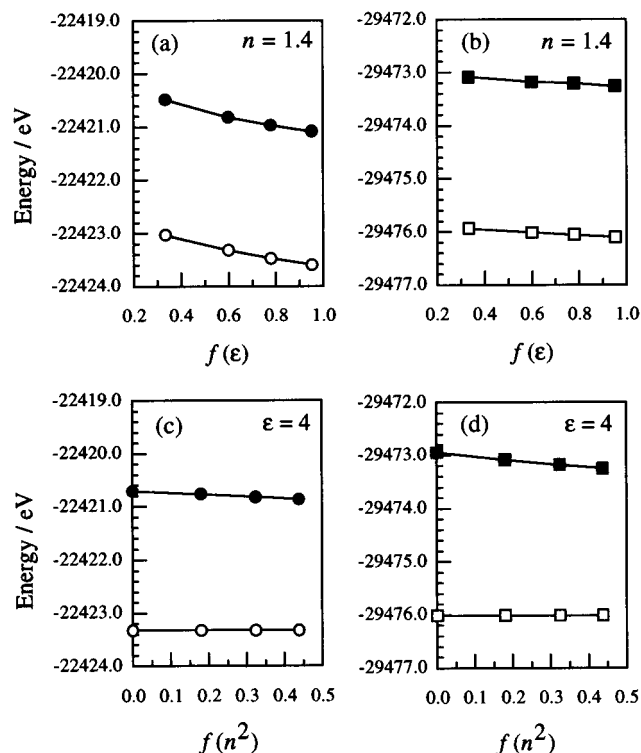


**Figure 11.** Energies of the ground state (○, □) and the  $\pi$ - $\pi^*$  excited state (●, ■) as a function of medium parameters. (a) and (c) are for **3a** (○, ●), and (b) and (d) are for **3b** (□, ■).

and lowest  $\pi$ - $\pi^*$  excited states on the medium parameters. The energies of these states of **3a** and those for **3b** are plotted as a function of  $f(\epsilon)$  ( $n$  is fixed to be 1.4) in Figure 11a,b, where the excited-state energy is the sum of the ground-state energy and the excitation energy obtained by the CI calculation. As for **3a** (Figure 11a), the increase in  $\epsilon$  lowers the energy of the ground state. This effect corresponds just to that of the counterion of PRSB. On the other hand, for the case of **3b** (see Figure 11b), the effect of the static dielectric constant is less important, because the acetate anion already serves as a counterion. In both **3a** and **3b**, the increase in  $\epsilon$  causes a lowering of the excited-state energy as well, but the amount of energy change is comparable to the solvation energy in the ground state. As a result, the slow relaxation of solvent, depending on static dielectric constant  $\epsilon$ , hardly affects the excitation energy in both cases of **3a** and **3b**. This supports the fact that in the PRSBs studied here the  $A$  values are much smaller than the  $B$  values.

In Figure 11c,d the electronic energies of the ground- and  $\pi$ - $\pi^*$  excited-states of **3a** and those of **3b** are plotted as a function of  $f(n^2)$  ( $\epsilon$  is fixed to be 4.0). As far as  $\epsilon$  is kept constant, the increase in  $n$  exerts no apparent influence on the ground-state energy. On the other hand, in both **3a** and **3b**, the increase in  $n$  causes a significant lowering of the excited-state energy, resulting in a red shift. This is just due to the external charge-like effect of the polarizable medium. In addition, the excited-state energies of **3a** and **3b** are lowered by 0.16 and 0.31 eV, respectively, with an increase in  $n$  from 1.0 to 1.6. This indicates that the polarizable medium operates more effectively for PRSB with a counterion (**3b**) than for the cationic form (**3a**). This explains why the  $B$  value for **3b** is larger than that for **3a** (Table 3).

According to the above analysis, the presence of counterion hardly affects the  $A$  value for PRSB, while it significantly increases the absolute value of  $B$ . These facts imply that the

coefficients  $A$ ,  $B$ , and  $C$  in eq 9 depend on the distance  $d$ , regarded as a measure of the counterion effect, in their respective ways. Now we attempt to find a functional form representing the  $d$ -dependence of these coefficients, namely  $A(d)$ ,  $B(d)$  and  $C(d)$ . For this purpose, it is sufficient to know how the absorption maximum of PRSB is influenced by the change of  $d$  for a given set of ( $\epsilon$ ,  $n$ ). Such information is obtained from the data for **6a-f**, which have different  $d$  values. As shown in Figure 9b, the absorption maxima of **6a-f** well fit the quadratic regression curve against  $1/d^2$ , when the medium parameters are specified. Thus, the following relationship should be satisfied

$$X(d) = \beta(1/d^2)^2 + \gamma(1/d^2) + \alpha \quad (15)$$

where  $X$  is  $A$ ,  $B$ , or  $C$ , and  $\alpha$ ,  $\beta$ , and  $\gamma$  are constants. Although it is not easy to determine the values of  $\alpha$ ,  $\beta$ , and  $\gamma$ , we can obtain the first-order approximation of eq 15 for each of  $A$ ,  $B$ , or  $C$ . For the coefficient  $C$ , we have already derived eq 13, which clearly indicates that the leading term of the right-hand side is  $\gamma(1/d^2)$ . For the coefficient  $A$ , the  $d$ -dependence is nearly negligible, because the  $A$  value is hardly affected according to whether PRSB has a counterion or not. Thus, the term  $\alpha$  is the leading term for  $A$ . Finally, to reproduce the quadratic nature of curves shown in Figure 9b, the coefficient  $B$  must exhibit a quadratic dependence on  $1/d^2$ . In other words, the leading term for  $B$  is  $\beta(1/d^2)^2$ , which is qualitatively consistent with the fact that the  $B$  value is most remarkably affected by the presence of a counterion. These relationships are useful for understanding the gross tendency of the concerted effect of counterion and medium.

A phenomenological feature of the above concerted effect becomes noticeable in media with high refractive indices. When  $n = 1.4$ – $1.6$ , the blue-shift induced by the counterion effect and the red-shift induced by the medium effect are almost compensated for each other in the region of  $0.00$ – $0.05$  of  $1/d^2$  (i.e.,  $d > 4.5$ ). Therefore, the absorption maxima of **6a-e** hardly depends on the location of their counterion in high-refractive index environments. According to our estimation based on eq 14, the retinal-binding pocket of bR, probably of Rh as well, satisfies this condition. **6b** is similar to the active center model of Rh proposed by Smith et al.,<sup>29</sup> who attempted to determine the spatial arrangement of a carboxylate group so as to reproduce the observed absorption maxima of this protein. To one's regret, the model was deduced from the calculation that did not involve the polarizable medium effect of the protein. The use of the in vacuo calculation may be inappropriate for a precise modeling of the protein.

The absorption maximum of **6f** keeps blue-shifted relative to those of **6a-e**. This implies that its solvatochromic shift is dominated by the contribution of  $C$ , namely the term proportional to  $1/d^2$ . Such an anomaly results from the fact that the distance  $d$  ( $3.5$  Å) of **6f** is significantly shorter than those of the others.

## Concluding Remarks

The present study demonstrated that the SCRF-CI method developed by us is a powerful tool for interpreting the solvatochromic shifts of *all-trans*-retinal, *all-trans*-RSB, and *all-trans*-PRSB. With the aid of this method, we succeeded in quantitatively reproducing the opsin shifts of bR<sub>568</sub> and M<sub>412</sub>. The calculation also revealed the contributions of all the mechanisms which had been believed to cause the opsin shift: namely, (1) ring/chain coplanarization, (2) weak interaction

between PRSB and its counterion, (3) the external charge effect, and (4) the polarizable medium effect of the protein matrix. Although mechanism (4) has been accepted only as a conceptual model, the present study provide a realistic picture on it. Explicit treatment of mechanism (4) enables us to reproduce not only the opsin shifts for bR<sub>568</sub> and M<sub>412</sub> but also the data for the artificial pigments and Rh. In conclusion, the aromatic residues forming the retinal-binding pocket plays a decisive role in causing the opsin shift. Finally, we must emphasize that such an unambiguous conclusion comes from the fact that the hexane

solution of PRSB was chosen as the reference state to measure the opsin shift.

**Acknowledgment.** The authors gratefully thank the Computer Center, Institute for Molecular Science, Okazaki, Japan, for the use of an NEC SX-3 supercomputer. They also thank the Computer Center, Tokyo Institute of Technology, Tokyo, Japan, for the use of a Cray C916 system.

JA973941T